Drug Design, Development and Therapy

Dovepress
open access to scientific and medical research

Open Access Full Text Article

ORIGINAL RESEARCH

Icariin and Competing Endogenous RNA Network: A Potential Protective Strategy Against Contrast-Induced Acute Kidney Injury

Yan Lin[1,2,*], Gaofeng Zhu[3,*], Xiaoyong Li[4,*], Huaxiao Yu[5], Yuhang Luo[5], Jiaqiong Lin[6], Renyuan Li[7], Zena Huang[2]

[1]Department of Nephrology, The Third Affiliated Hospital of Guangzhou Medical University, Guangzhou, People's Republic of China; [2]Yunkang School of Medicine and Health, Nanfang College, Guangzhou, People's Republic of China; [3]Department of General Medicine, Guangdong Provincial People's Hospital, Guangdong Academy of Medical Sciences, Guangzhou, People's Republic of China; [4]Department of General Surgery, The Third Affiliated Hospital of Guangzhou Medical University, Guangzhou, People's Republic of China; [5]The Third Clinical School, Guangzhou Medical University, Guangzhou, People's Republic of China; [6]Affiliated Dongguan Maternal and Child Healthcare Hospital, Southern Medical University, Guangzhou, People's Republic of China; [7]Department of Endocrinology and Metabolism, The Third Affiliated Hospital of Guangzhou Medical University, Guangzhou, People's Republic of China

*These authors contributed equally to this work

Correspondence: Zena Huang, Yunkang School of Medicine and Health, Nanfang College, Guangzhou, People's Republic of China, Tel +86-13570466614, Email huangzn@nfu.edu.cn; Renyuan Li, Department of Endocrinology and Metabolism, The Third Affiliated Hospital of Guangzhou Medical University, Guangzhou, People's Republic of China, Tel +86-18926146852, Email lirenyuan@gzhmu.edu.cn

Background: Icariin presents protective effect in several kidney diseases. However, the role of icariin in contrast-induced acute kidney injury (CIAKI) is still unclear. This study aimed to investigate the effect of icariin in CIAKI, as well as exploring the underlying mechanism from the aspect of interaction between protein-coding genes and non-coding RNAs.

Methods: The effect of icariin was evaluated in both in vivo and in vitro CIAKI models. Rat kidneys were collected for genome-wide sequencing. The differentially expressed genes (DEGs) were screened and visualized by R software. The function annotation of DEGs was analyzed by Metascape. By Cytoscape software, the competing endogenous RNA (ceRNA) network was constructed, and hub genes were selected. Expressions of hub genes were validated by PCR. Association of hub genes in the ceRNA network and renal function was also examined.

Results: Icariin protected against CIAKI in both in vivo and in vitro models. Based on DEGs in icariin pretreated CIAKI rats, lncRNA- and circRNA-associated ceRNA networks were constructed, respectively. Function annotation showed the ceRNA networks were enriched in ERK1 and ERK2 cascade, MAPK signaling and NF-κB signaling. Further, two circRNAs, six lncRNAs, four miRNAs and nine mRNAs were selected as hub genes of the ceRNA network. Among them, eight mRNAs (Acot1, Cbwd1, Ly6i, Map3k14, Mettl2b, Nyap1, Set and Utp20) were negatively correlated with renal function, while one mRNA (Tmem44) was positively correlated with renal function.

Conclusion: Icariin presented a protective effect against CIAKI. The ceRNA network, involving Acot1, Cbwd1, Ly6i, Map3k14, Mettl2, Nyap1, Set, Tmem44 and Utp20, might partially contribute to the underlying mechanism of icariin protection by regulation of ERK1 and ERK2 cascade, MAPK signaling and NF-κB signaling.

Keywords: icariin, contrast medium, acute kidney injury, competing endogenous RNA, non-coding RNA

Background

Contrast induced acute kidney injury (CIAKI) is characterized by development of acute kidney injury (AKI) after intravascular administration of contrast medium (CM).[1] The Kidney Disease Improving Global Outcome (KDIGO) working group suggested a definition based on a plasma creatinine (Cr) level or a urinary volume, which is increase of Cr by no less than 1.5 times within 7 days or by at least 0.3mg per deciliter within 48 hours after exposure to CM, or decrease of urinary volume to less than 0.5 mL per kilogram of body weight per hour that persists for at least 6 hours

Received: 12 April 2022
Accepted: 10 July 2022
Published: 23 July 2022

after exposure.[2] Many studies have shown that CIAKI is associated with severe adverse outcomes, including increased mortality[3] and progression of underlying chronic kidney disease.[4] However, preventive strategies of CIAKI in current practice are far from satisfying. The benefits of most pharmaceutical agents are still unconvincing,[5] and the protective effect of intravenous fluids is also challenged by a recent study.[6] Thus, it is urgent to develop a reliable preventive strategy for CIAKI in the large and growing population undergoing contrast enhanced procedures.

Epimedii Herba is a herbal medicine originating from *Epimedium koreanum Nakai, Epimedium brevicornum Maximowicz*, E*pimedium pubescens Maximowicz*, or E*pimedium sagittatum Maximowicz*. It is treated as a "kidney-tonifying" agent in traditional Chinese medicine.[7] Icariin, a major flavonoid responsible for the pharmacological actions of *Epimedii Herba*,[8] has shown promising protection in several kidney diseases, including cisplatin-induced cytotoxicity,[9] ureteral obstruction[10] and diabetic nephropathy.[11] Icariin carries out renal protection by multiple biological activities, such as anti-inflammation,[12] anti-oxidative stress,[9,11] restoring autophagy[11] and inhibition of NF-κB pathway.[13] However, the potential effect of icariin in CIAKI has not been investigated so far.

Non-coding RNAs (ncRNAs) are transcripts with no or low coding potential, among which microRNAs (miRNAs), long non-coding RNAs (lncRNAs) and circular RNAs (circRNAs) attract most attention in current researches. Emerging evidence has indicated that ncRNAs are important in renal biological maintenance and pathophysiological process.[14] LncRNAs, circRNAs and mRNAs may compete to bind to same miRNA, an association known as the competing endogenous RNA (ceRNA) mechanism.[15] An amount of studies has shown that, by forming a ceRNA network with mRNAs, ncRNAs can affect the pathogenesis and therapeutic response of kidney diseases. Several ceRNA networks are identified in CIAKI rat models,[16] while the underlying mechanism of ceRNA networks in prevention of CIAKI is still ambiguous.

In the present study, we first investigated the effect of icariin in CM treated rats and human renal tubular epithelial cells. Then we analyzed the expression profile and function annotation of mRNAs, miRNAs, lncRNAs and circRNAs based on next generation RNA sequencing. Further, we constructed an icariin-associated ceRNA network and identified key modules in the network. Finally, we assessed the correlation of key modules in ceRNA network and renal function. Our findings revealed that icariin showed profound protection against CIAKI via ceRNA network, providing a potential preventive strategy for CIAKI.

Methods

Materials

Icariin, with a purity of 98%, was purchased from Glpbio Technology (CA, USA, Cat. No.: GN10278). A type of nonionic low-osmolar contrast medium iopromide (Ultravist 370, 370 mg/mL iodine), purchased from Bayer HealthCare LLC (Leverkusen, Germany), was used as the iodinated radiographic contrast agent. Furosemide was bought from Glpbio Technology (CA, USA, Cat. No.: GC12970). Human renal tubular epithelial cell lines, HK-2 cells, were bought from Procell Life Science & Technology Co. (Wuhan, China). The RNA isolation reagent Trizol and cDNA synthesis kit were bought from TaKaRa Bio. (Tokyo, Japan). Dulbecco's modified Eagle's medium (DMEM), fetal bovine serum and PBS buffer were purchased from Gibco Life Technologies (NY, USA). The cell counting kit-8 (CCK-8) test solution was bought from Dojindo Lab. (Japan). The TUNEL assay was purchased from Beyotime Bio. (Shanghai, China, Cat. No.: C1088).

Construction of in vivo CIAKI Model and Pretreatment with Icariin

All animal experiments were approved by Guangzhou Medical University and conducted in accordance with the US guidelines (NIH publication #85-23, revised in 1985). Mature male Sprague–Dawley rats, weighing 180–200 g, were chosen for this experiment. They were housed under controlled conditions of light (12 h/12 h light/dark cycle) and temperature (21–23°C) and allowed free access to standard laboratory diet and water. Rats were divided into three groups, while there are eight rats in each group: (1) control group: rats received saline solution at each time point; (2) CIAKI group: rats established CIAKI protocol; (3) CIAKI + icariin group: before establishment of CIAKI protocol, rats received icariin (100 mg/kg, in saline with a concentration of 1%) intragastrically once daily for three

consecutive days. The dosage of icariin was determined according to previous studies.[17,18] CIAKI protocol was established based on previous studies.[19] Briefly, furosemide was administrated intragastrically at 200 mg/kg and dehydration for 6h before the contrast medium was injected at 15mL/kg by tail vein. After contrast administration, rats were allowed free access to water. Twenty-four hours after CIAKI protocol establishment, rats were weighed and obtained blood samples from orbital vein. And then the rats were killed under anesthesia (chloral hydrate (400 mg/kg, i.p.)). The kidneys were separated from renal capsules and weighed in the equatorial plane; one kidney was dissected and kept in liquid nitrogen for high throughput sequencing analysis, and the other was fixed in phosphate-buffered 4% formalin and prepared for histological examination.

Evaluation of Biochemical Parameters

Mean serum Cr, blood urea nitrogen (BUN) and Cystatin C (Cys-C) concentrations were measured using automatic biochemistry analyzer at the Clinical Laboratory, The Third Affiliated Hospital of Guangzhou Medical University.

Histological Examination of Renal Tissues

Kidney sections of 4μm were obtained from paraffin-embedded samples and subjected to hematoxylin and eosin (HE) staining and Periodic Acid-Schiff (PAS) staining. For semiquantitative analysis of morphological changes, 10 high-magnification (×200) fields of the cortex and outer stripe of the outer medulla were randomly selected. The tubular injury was evaluated according to the following criteria: tubular dilatation and necrosis, brush border loss and proteinaceous casts. Damage was graded on a scale from 0 to 4: 0, no abnormalities; 1+, damage less than 25%; 2+, damage between 25 and 49%; 3+, damage between 50 and 74%; 4+, damage more than 75%. The average score of 10 fields was used for each kidney sample.[20] TUNEL assay was performed on paraffin-embedded kidney tissue to present apoptotic DNA fragmentation. Counterstained with DAPI, the apoptotic cells (FITC positive) appeared brightly green in color after fluorescent staining. For quantitative analysis, TUNEL-positive cells were analyzed in six random high-magnification (×400) fields using the Particle Analyzer function in ImageJ.[21]

RNA Extraction and Qualification

Three rats from each group were randomly chosen for whole-genome sequencing. Total RNA from each kidney was extracted using TRIzol reagent (Thermo Fisher Scientific, MA, USA) according to the manufacturer's instructions. One percent agarose gels were used for RNA degradation and contamination. RNA concentration was measured using a Qubit RNA Assay Kit in a Qubit 2.0 Fluorometer (Life Technologies, CA, USA). RNA integrity was assessed using the RNA Nano 6000 Assay Kit with the Agilent Bioanalyzer 2100 system (Agilent Technologies, CA, USA).

RNA Sequencing

All sequencing programs were carried out by Biomarker Company (Beijing, China). In brief, gene expression profiling of genome-wide kidney tissues was performed using RNA deep sequencing. Moreover, library construction was performed following the manufacturer's instructions (Illumina, San Diego, CA). Samples were sequenced on an Illumina HiSeq 2500 instrument.

Bioinformatics

Bioinformatic analysis was performed by R language (version 3.4.4). The raw read counts of genes were normalized, and then transcripts per million (TPM) was applied. Differentially expressed genes (DEGs) were analyzed by "DeSeq2", while absolute value of fold change (FC) $\geq$ 1.5 and adjusted $p < 0.05$ was considered significant. Then, the "EnhancedVolcano" and "pheatmap" packages were used to draw volcano maps and heatmaps. Gene Ontology (GO) analysis of differentially expressed (DE) mRNAs was achieved by Metascape web server.[6] Predicted target genes were filtered by miRDB (http://mirdb.org/), Targetscan (http://www.targetscan.org/), circBase (http://www.circbase.org) and Lncpedia (https://lncipedia.org) databases. The ceRNA network was constructed based on DEGs. The cross-linking relationship and network construction were performed by Cytoscape version 3.6.0. For mRNAs in the ceRNA network,

WebGestalt online tool (http://www.webgestalt.org) were utilized for function annotation, while another online tool String[22] were used for protein–protein interaction (PPI) prediction. "Cytohubba" plug-in of Cytoscape was applied to identify key modules of the ceRNA network. "Ggalluvial" package was used for visualization of the ceRNA network as a Sankey plot. Based on the median level of Map3k14, the nine sequenced rats were divided into two groups. Then, Map3k14 associated GSEA analysis was carried out by WebGestalt online tool. "Corrplot" package was used for correlation analysis of renal function and key modules in the ceRNA network. The fitting curves of Cr and specific modules were exhibited by GraphPad Prism 9 software.

RNA Isolation and PCR Amplification

The total RNA was isolated from the kidney using Trizol. Reverse transcription into cDNA was performed using a PrimeScript II 1st Strand cDNA synthesis kit. The real-time quantitative PCR amplification was done by Power SYBR Green PCR Master Mix (Thermo Fisher). 50°C for 2 min, 95°C for 2 min, 40 cycles of 95°C for 15s, 60°C for 1min were set as the reaction conditions. The primers used were listed in Table S1. The relative expression levels were calculated using the $2^{-\Delta\Delta Ct}$ methods.

In vitro Study of Icariin Protection in CM-Induced Renal Tubular Injury

HK-2 cells were preserved in DMEM with 10% fetal bovine serum under a condition of 37°C and 5% CO_2 atmosphere. The culture medium was replaced with fresh medium every 2–3 days. The cells were expanded to new culture plates when about 80% confluent. HK-2 cells were exposed to CM at different concentrations for individual times to investigate its injury. In order to assess the effect of icariin against CM-induced injury, HK-2 cells were co-treated with icariin at different concentrations when exposed to CM.

The cell viability was detected by CCK-8 assay. The HK-2 cells were incubated in 96-well plate at a concentration of 1×10^4 cells/mL at 37°C. After indicated treatments, the cells were washed twice with PBS. Then the cells were incubated with 10μL CCK-8 test solution and 90 mL DMEM at 37 °C for 2 h. The optical density (OD) was measured by absorbance value at the 450nm wavelength using a microplate reader (Molecular Devices, USA). The mean of the OD of three wells in each group was used for calculation of cellular activity percentage, according to the following formula: cell viability (%) = (OD of treatment group/OD of control group) × 100%.

Statistical Analysis

All data were expressed as the mean ± SD. Differences between groups were determined by one-way analysis of variance (ANOVA) using SPSS 17.0 software (SPSS, Inc, Chicago, IL, USA) followed by the least significant difference (LSD) post hoc comparison test. Differences were considered statistically significant at $p < 0.05$.

Results

Icariin Protected Against CIAKI in in vivo and in vitro Models

In Sprague–Dawley rats, iopromide caused significant elevation of serum Cr (Figure 1A), BUN (Figure 1B) and Cys-C (Figure 1C) levels. Prominent morphological changes, such as tubular dilatation and necrosis, proteinaceous casts and interstitial edema, were also observed in iopromide treated rat kidneys (Figure 1D and E). However, icariin pretreatment exhibited remarkable renal protection in CIAKI rats, as it alleviated serum Cr, BUN and Cys-C expressions (Figure 1A–C) and ameliorated morphological injury (Figure 1D and E). Moreover, icariin could dampen iopromide-induced renal apoptosis, presented as decreased TUNEL-positive renal tubular cells (Figure 1F and G).

In HK-2 cells, iopromide caused dose (Figure 2A) and time (Figure 2B) dependent injury. As iopromide with a concentration of 150 mg I/mL treating for 9 h could induce nearly 40% cell death, it was set as the CM-induced renal tubular injury model. Next, we tested the effect of icariin on cell viability alone. As shown in Figure 2C, icariin did not decrease cell viability in the concentration lower than 100 μM, which was then used for the following investigation. Further, we explored the effect of icariin in CM-induced renal tubular injury model. In Figure 2D, icariin could

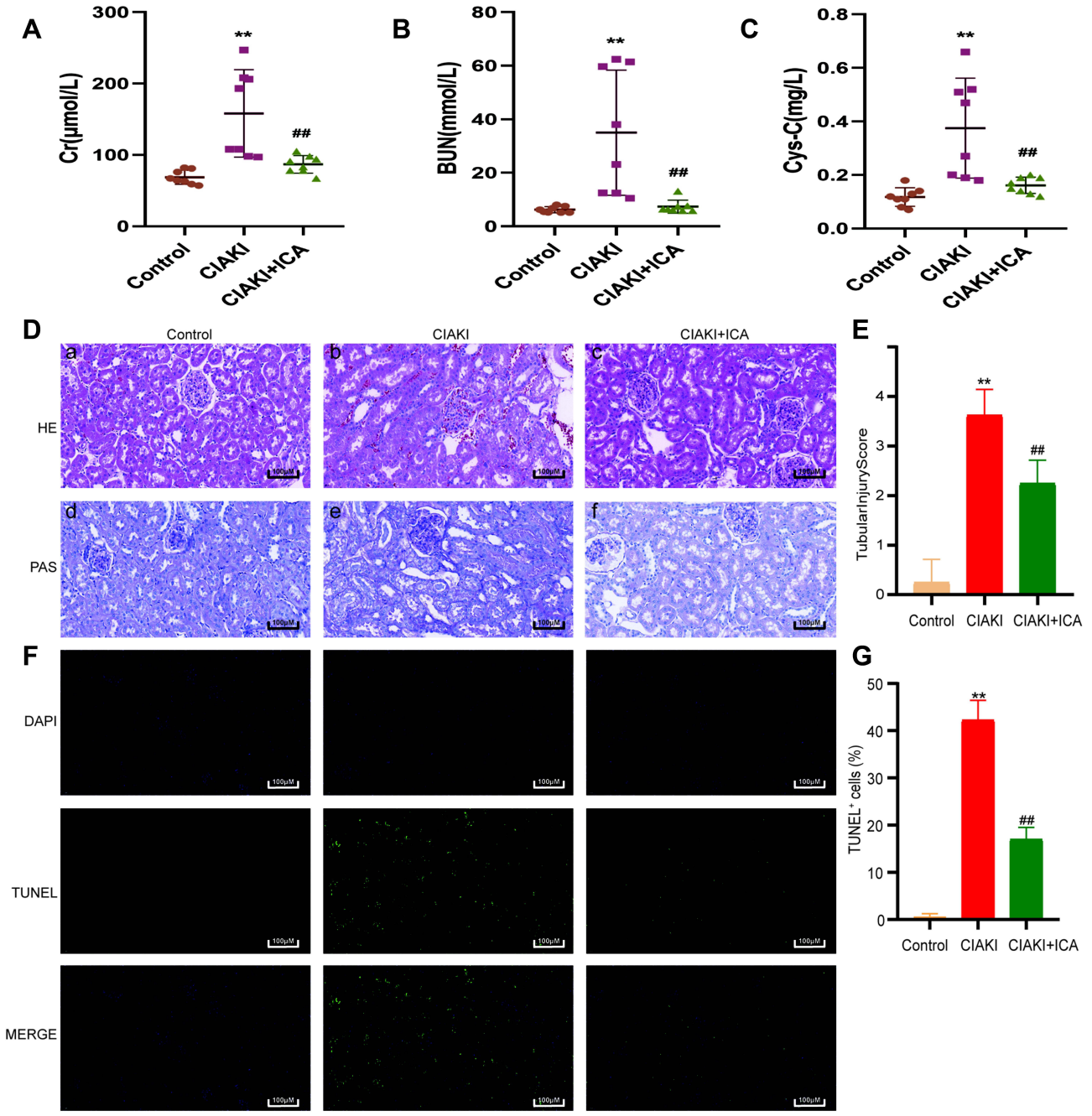

Figure 1 Icariin protected against iopromide-induced AKI in in vivo studies. The levels of Cr (**A**), BUN (**B**) and Cys-C (**C**) were compared among control group, CIAKI group and CIAKI+icariin group. The histological characteristics were shown by HE and PAS stained kidney sections (**D**). Moreover, the semiquantitative tubular injury score was evaluated (**E**). TUNEL staining was also applied to investigate renal tubular apoptosis (**F** and **G**). $^{**}p < 0.01$ vs control group; $^{\#\#}p < 0.01$ vs CIAKI group.

remarkably attenuate CM-induced renal tubular cell death in the concentration from 1 to 50 μM. The above data indicate a prominent protective effect of icariin against CIAKI in both in vivo and in vitro models.

Identification of DEGs in Icariin Pretreated CIAKI Rats

Next, we randomly chose three rats from each group, and carried out next-generation sequencing to the kidney tissues. Overview of gene expression in these nine rat kidneys is shown in Figure S1. Totally, there are 4348 DE mRNAs (Figure 3A), 149 DE miRNAs (Figure 3D), 1082 DE lncRNAs (Figure 3G) and 19 DE circRNAs (Figure 3J) between control and CIAKI group. Moreover, there are 3975 DE mRNAs (Figure 3B), 128 DE miRNAs (Figure 3E),

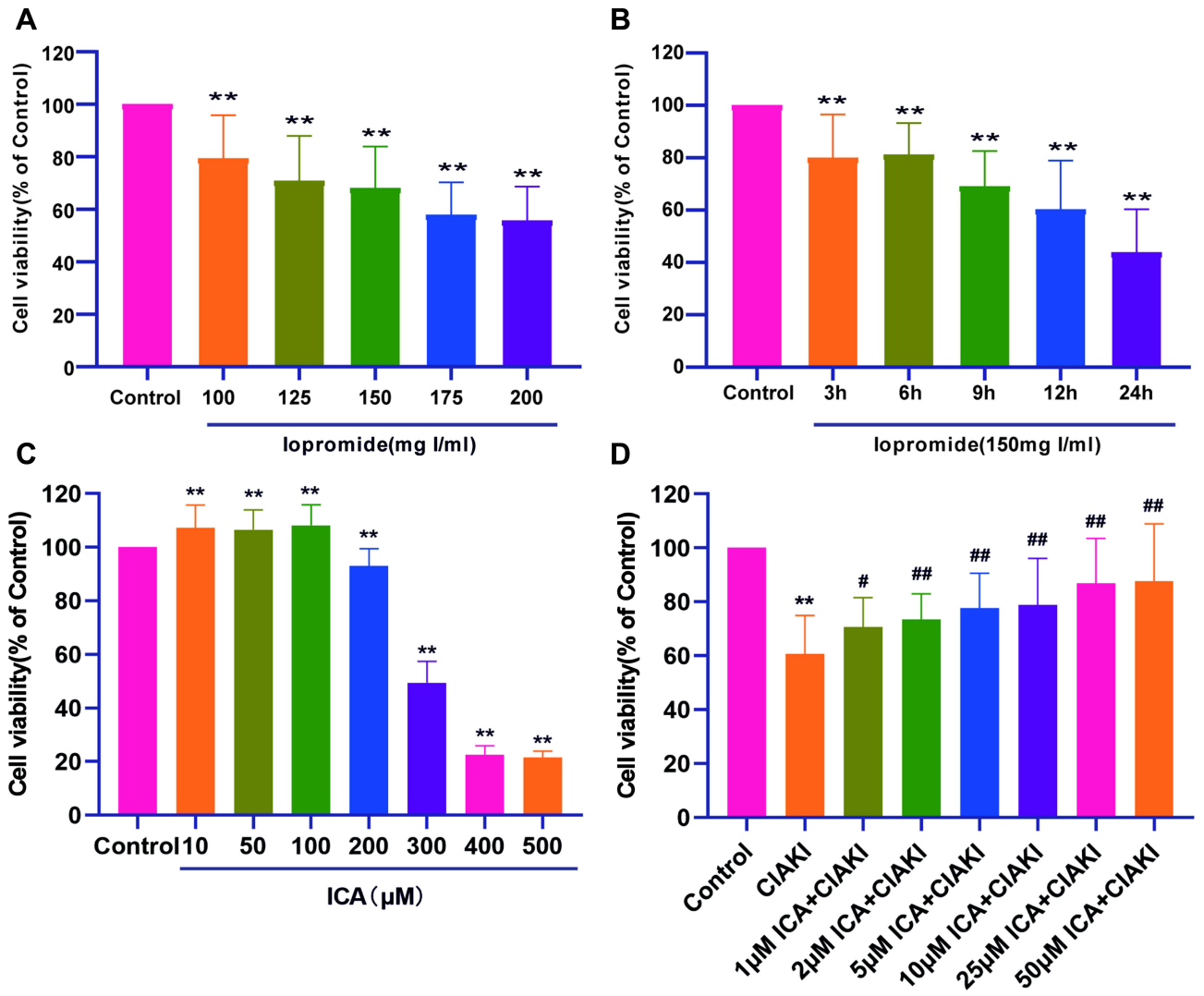

Figure 2 Icariin ameliorated iopromide-associated damage and apoptosis in proximal tubular epithelial cell. Iopromide induced dose (**A**) and time (**B**) dependent injury to HK-2 cells. The effect of icariin on cell viability was detected next, and the concentration below 100 μM was selected for further study (**C**). HK-2 cells were co-treated with CM and icariin in different concentrations to explore the protective effect of icariin against CM-induced tubular injury (**D**). $^{**}p < 0.01$ vs control group; $^{\#}p < 0.05$ vs CIAKI group; $^{\#\#}p < 0.01$ vs CIAKI group.

989 DE lncRNAs (Figure 3H) and 16 DE circRNAs (Figure 3K) between CIAKI and CIAKI+icariin group. The distribution of DEGs was also exhibited by circos plots (Figure S2A and S2C) and pie charts (Figure S2B and S2D). More details of DEGs were displayed in Tables 1–4. To further investigate genes attributed to icariin protection against CIAKI, we looked for DEGs with similar expression trends in control group and CIAKI+icariin group. Finally, we focused on 3112 mRNAs (Figure 3C), 62 miRNAs (Figure 3F), 396 lncRNAs (Figure 3I) and 5 circRNAs (Figure 3L).

Function Annotation of DEGs in Icariin Pretreated CIAKI Rats

To clarify the biological function of DE mRNAs, gene ontology (GO) annotation was conducted by Metascape. In Figure 4A, top 20 enriched GO terms were presented by a heatmap. DEGs from CIAKI group and CIAKI+icariin group were both enriched in response to drug (GO: 0042493), inflammatory response (GO: 0006954), response to wounding (GO:0009611) and Nrf-2 signaling (WP2376). Top 100 enriched GO terms were also exhibited in Figure S3. To better display the correlation in biological function between CIAKI and CIAKI+icariin groups, enriched GO terms were

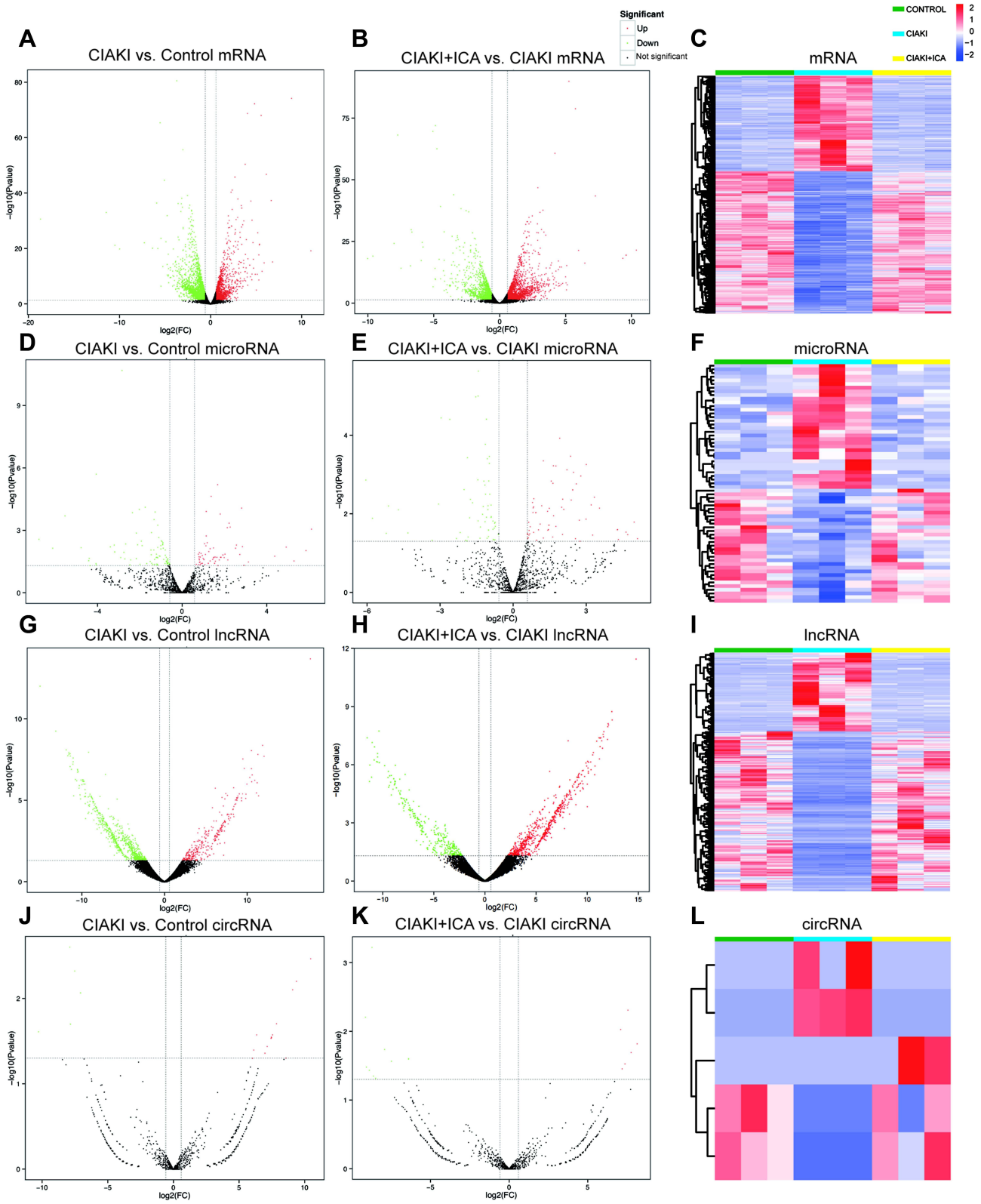

Figure 3 Expression profile of DEGs in CIAKI rats, with and without icariin pretreatment. Volcano maps for mRNA (**A** and **B**), miRNA (**D** and **E**), lncRNA (**G** and **H**) and circRNA (**J** and **K**) were presented between control group and CIAKI group, as well as between CIAKI group and CIAKI+icariin group. The green dot stands for significantly down regulated genes, the red dot stands for significantly up regulated genes, and the black dot stands for not significant genes. $|FC| \geq 1.5$ and $p < 0.05$ was treated as significant. The overall expression profiles among the three groups were also shown by heatmaps (**C, F, I** and **L**). The elevated genes were in red color, and the decreased genes were in blue color. CIAKI+ICA group: CIAKI rats with icariin pretreatment.

https://doi.org/10.2147/DDDT.S369100 DovePress

Table 1 Top 20 Differentially Expressed mRNAs

Gene Symbol	Log_2 FC	*P* value	FDR	Regulated
CONTROL vs CIAKI				
Cyp3a9	11.0278543	6.61E-20	2.13E-18	Up
Grm8	−9.9736924	1.53E-20	5.20E-19	Down
Havcr1	8.89827255	5.67E-75	1.23E-71	Up
Angptl4	6.13867342	1.54E-47	7.44E-45	Up
Sphkap	−5.9023721	3.70E-37	8.47E-35	Down
RGD1561212	5.88791402	1.58E-15	3.11E-14	Up
Gpnmb	5.57799192	9.51E-69	8.27E-66	Up
Slc7a11	5.39792071	2.77E-22	1.17E-20	Up
LOC299282	5.37814298	4.38E-22	1.73E-20	Up
Trim15	5.3123989	2.04E-09	1.43E-08	Up
Cxcl9	−5.2406064	2.84E-14	4.57E-13	Down
Creb3l3	5.19615946	1.99E-26	1.33E-24	Up
Abcc2	4.85196316	6.14E-73	8.90E-70	Up
AC118957.1	4.7377126	1.08E-13	1.61E-12	Up
Ucma	4.70629106	7.47E-17	1.71E-15	Up
Prima1	−4.6396449	1.14E-18	3.26E-17	Down
Fam163a	−4.593878	2.15E-08	1.19E-07	Down
Akr1b7	4.57448773	1.66E-11	1.71E-10	Up
Igfbp1	4.5569859	5.47E-31	5.80E-29	Up
Glycam1	4.55110641	1.88E-09	1.33E-08	Up
CIAKI vs CIAKI+ICA				
Grm8	9.60888224	3.34E-20	1.34E-18	Up
AABR07037356.1	−8.0059711	6.07E-25	4.64E-23	Down
Havcr1	−7.721897	6.82E-69	5.4253E-66	Down
Cyp3a9	−7.4759622	6.24E-15	1.22E-13	Down
RGD1561212	−5.9449313	4.52E-18	1.37E-16	Down
Slc7a11	−5.8688649	2.10E-25	1.71E-23	Down
Ugt2a3	−5.8147911	1.67E-23	1.07E-21	Down
Gpnmb	−5.0570331	2.07E-70	2.05E-67	Down
Fgg	−4.8894175	8.08E-15	1.54E-13	Down
Abcc2	−4.8549926	9.11E-73	1.21E-69	Down
Foxn4	4.78938836	8.20E-09	5.78E-08	Up
Fgb	−4.7581718	2.59E-63	1.72E-60	Down
Angptl7	4.69323371	2.10E-15	4.32E-14	Up
Lilrb3	4.67011952	2.32E-08	1.45E-07	Up
PVR	−4.5883255	1.43E-18	4.66E-17	Down
Prima1	4.55924896	2.09E-15	4.32E-14	Up
Sphkap	4.48611192	9.45E-09	6.57E-08	Up
Tnfrsf12a	−4.4707902	6.29E-40	2.27E-37	Down
Lrtm2	4.45043841	1.02E-07	5.33E-07	Up
Ano2	4.45016144	6.80E-18	2.02E-16	Up

clustered as a network further. Combing Figure 4B and C, overlapped GO terms enriched in inflammatory response, leukocyte migration, response to wounding and Nrf-2 signaling might be part of the underlying mechanism in icariin protection against CIAKI. Specific information of top enriched GO terms is demonstrated in Table 5.

Table 2 Top 20 Differentially Expressed microRNAs

Gene Symbol	Log_2 FC	*P* value	FDR	Regulated
CONTROL vs CIAKI				
novel_miR_926	−6.7642153	0.00269773	0.17980985	Down
novel_miR_70	6.1284514	0.00087167	0.07423736	Up
rno-miR-741-3p	−6.1079022	0.0070925	0.23481394	Down
novel_miR_930	5.86089378	0.00937366	0.27112861	Up
novel_miR_1021	−5.5259289	0.00020148	0.02573844	Down
novel_miR_350	5.29298252	0.02966469	0.42361654	Up
rno-miR-3590-3p	4.92389621	0.0064522	0.23481394	Up
novel_miR_690	−4.7674164	0.00674869	0.23481394	Down
novel_miR_856	−4.4145096	0.02822783	0.41608902	Down
novel_miR_230	−4.3924705	0.02199036	0.38308203	Down
rno-miR-501-5p	4.37976668	0.01752773	0.37013001	Up
novel_miR_675	−4.3532177	0.04904395	0.50122921	Down
novel_miR_270	−4.0610443	0.03968298	0.4727396	down
novel_miR_327	−4.0553435	0.04546494	0.47994193	Down
novel_miR_735	−4.0548866	2.00E-06	0.00153652	Down
novel_miR_478	−3.3831976	0.00617938	0.23481394	Down
novel_miR_285	−3.1992659	0.00499936	0.22223092	Down
novel_miR_342	−3.1770068	0.01088491	0.29274683	Down
novel_miR_64	−3.1769727	0.0108408	0.29274683	Down
novel_miR_879	−3.1768954	0.01074107	0.29274683	Down
CIAKI vs CIAKI+ICA				
novel_miR_70	−6.0393277	0.00138362	0.08851203	Down
novel_miR_930	−5.7714473	0.01292285	0.29507179	Down
novel_miR_350	−5.2057501	0.03115884	0.4773146	Down
novel_miR_592	−5.118717	0.00629929	0.20637018	Down
novel_miR_117	5.10732685	0.04300895	0.54491693	Up
novel_miR_583	4.9700881	0.01620513	0.33476182	Up
rno-miR-296-5p	4.70897517	0.03357356	0.4773146	Up
novel_miR_761	−4.7059945	0.00786248	0.21543188	Down
novel_miR_1021	4.63706511	0.02922968	0.46860782	Up
novel_miR_759	4.32815351	0.04517624	0.55802946	Up
novel_miR_992	−4.3163155	0.03068124	0.47666623	Down
novel_miR_690	4.29359773	0.02518674	0.42508062	Up
novel_miR_176	4.29359235	0.02516188	0.42508062	Up
novel_miR_190	4.2774548	0.02547567	0.42508062	Up
novel_miR_163	3.54885521	0.00711898	0.20921905	Up
novel_miR_1002	3.33888576	0.00375234	0.16631689	Up
novel_miR_484	−3.3213721	0.04720635	0.56392302	Down
novel_miR_394	3.27050095	0.03478393	0.48536467	Up
novel_miR_311	3.20813251	0.00593143	0.20637018	Up
novel_miR_6	−3.0611681	0.00564276	0.20637018	Down

Construction of Icariin-Associated ceRNA Networks in CIAKI Rats

In order to figure out the interaction between protein-coding genes and ncRNAs in icariin protection against CIAKI, we tried to construct ceRNA networks using the selected 3112 mRNAs, 62 miRNAs, 396 lncRNAs and 5 circRNAs. By cytoscape, we set up a lncRNA-associated ceRNA network (Figure S4), including 417 edges and 389 nodes (93 lncRNAs, 15 miRNAs and 281 mRNAs). We also set up a circRNA-associated ceRNA network (Figure S5), including 277 edges and 264 nodes (4 circRNAs, 8 miRNAs and 252 mRNAs). Each ceRNA network

Table 3 Top 20 Differentially Expressed lncRNAs

Gene Symbol	Log_2 FC	*P* value	FDR	Regulated
CONTROL vs CIAKI				
mstrg.21296.10	17.6539327	2.03E-14	2.12E-11	Up
MSTRG.7795.1	−15.020078	9.75E-13	5.28E-10	Down
MSTRG.16453.27	−13.119749	5.58E-10	2.01E-07	Down
MSTRG.19989.29	12.0438895	1.97E-08	1.53E-06	Up
MSTRG.45112.3	11.878735	4.30E-09	1.162E-06	Up
MSTRG.43827.2	−11.8624	8.03E-09	1.74E-06	Down
MSTRG.4074.11	−11.661532	1.82E-08	1.64E-06	Down
MSTRG.72327.5	−11.5576	1.16E-08	1.57E-06	Down
MSTRG.44351.2	−11.543148	1.45E-08	1.57E-06	Down
MSTRG.65323.2	−11.40177	8.39E-08	4.78E-06	Down
MSTRG.28471.13	−11.400525	1.40E-08	1.68E-06	Down
MSTRG.58281.3	11.3865787	5.25E-06	9.47E-05	Up
MSTRG.18441.20	−11.382525	1.93E-08	1.60E-06	Down
MSTRG.48297.7	11.3004683	1.54E-08	1.52E-06	Up
MSTRG.44067.9	−11.238788	1.26E-07	6.20E-06	Down
MSTRG.30953.4	11.2190659	8.26E-07	2.18E-05	Up
MSTRG.73438.1	11.14624	3.52E-06	7.46E-05	Up
MSTRG.56262.2	−11.060242	5.98E-08	3.60E-06	Down
MSTRG.61777.10	−11.037243	2.52E-08	1.82E-06	Down
MSTRG.33212.24	−11.03358	4.28E-08	2.72E-06	Down
CIAKI vs CIAKI+ICA				
MSTRG.7795.1	14.7896364	3.57E-12	3.53E-09	Up
MSTRG.72327.5	12.4370251	4.89E-09	1.61E-06	Up
MSTRG.23554.9	12.4208058	1.80E-09	8.89E-07	Up
MSTRG.28471.13	12.1003506	9.19E-09	1.82E-06	Up
MSTRG.51241.14	12.0433366	7.62E-09	1.88E-06	Up
MSTRG.34520.3	12.0181514	1.11E-08	1.82E-06	UP
MSTRG.37283.2	12.006093	5.10E-08	3.36E-06	Up
MSTRG.64950.25	11.6364935	2.05E-08	2.53E-06	Up
MSTRG.55356.2	11.5976363	3.64E-08	3.60E-06	Up
MSTRG.6581.104	11.5741194	2.82E-08	3.10E-06	Up
MSTRG.4074.11	11.5132098	1.44E-07	6.49E-06	Up
MSTRG.24032.13	−11.509949	4.12E-08	3.70E-06	Down
MSTRG.53408.13	11.4242866	5.96E-08	3.68E-06	Up
MSTRG.28471.11	11.3191455	4.13E-08	3.40E-06	Up
MSTRG.5249.1	−11.301525	7.36E-06	9.70E-05	Down
MSTRG.35484.10	11.2691801	1.18E-07	5.83E-06	Up
MSTRG.5597.2	11.2659783	4.35E-08	3.070E-06	Up
MSTRG.30953.4	−11.250942	1.04E-06	2.79E-05	Down
MSTRG.36664.18	11.1871286	5.07E-07	1.86E-05	Up
MSTRG.40033.6	11.1671782	4.14E-08	3.15E-06	Up

was divided into two parts, one with up-regulated miRNAs in CIAKI+icariin group, the other with down-regulated miRNAs.

Enrichment Analysis and PPI Analysis of Icariin-Associated ceRNA Networks

Further, we focused on the potential molecular mechanism and pathways of ceRNA networks participating in icariin protection against CIAKI. Using the WebGestalt online tool, we found icariin-associated ceRNA networks were highly

Table 4 Differentially Expressed circRNAs

Gene ID (Chromatin:Start|end)	Log_2 FC	*P* value	FDR	Regulated
CONTROL vs CIAKI				
2:88552337|88593717	10.470445	0.00338823	0.03218818	Up
2:88552337|88560196	−10.271976	0.02453005	0.05178566	Down
4:50180977|50200342	9.37214914	0.00624814	0.02967866	Up
10:13767446|13810899	9.07943813	0.00787247	0.02991538	up
1:221184324|221186464	8.57583381	0.04973633	0.05249946	UP
14:37238505|37262083	−7.8763705	0.00248906	0.04729214	Down
1:278580846|278620822	7.85615509	0.01970514	0.05348539	Up
1:278580846|278749829	−7.8328111	0.019,98953	0.04747514	Down
9:71954951|71960153	7.54896702	0.02659429	0.05052914	Up
4:66172555|66200637	−7.5127959	0.00473452	0.02998529	Down
12:40329454|40332371	7.47448871	0.02834381	0.0448777	Up
9:73752937|73799430	7.46872509	0.02885535	0.0421732	Up
2:238023879|238038227	7.43970127	0.02932584	0.03979935	Up
19:22143683|22179584	7.1556389	0.03644567	0.04616451	Up
8:43806521|43816234	−7.0637788	0.00857427	0.02715186	Down
17:5555491|5571375	6.97290956	0.04356533	0.04869066	Up
5:161794861|161799241	6.34430518	0.02664314	0.04601997	Up
18:59190041|59192425	6.12233855	0.04022876	0.04777165	Up
13:101502509|101503027	6.02832571	0.04998717	0.04998717	Up
CIAKI vs CIAKI+ICA				
10:13767446|13810899	−9.1243622	0.00617372	0.0329265	Down
4:68897362|68967998	−9.0650588	0.03293919	0.04391892	Down
1:168958579|168964665	−8.8786727	0.03677901	0.04203316	Down
1:278580846|278594581	−8.7142767	0.00059575	0.00953206	Down
1:221184324|221186464	−8.6207115	0.0444879	0.04745376	Down
3:177390074|177433646	−8.4730625	0.04786317	0.04786317	Down
1:278580846|278749829	8.14658415	0.01519001	0.04860804	Up
1:278580846|278620822	−7.900979	0.01831919	0.04885118	Down
6:136059672|136084622	7.76182285	0.02035657	0.04652931	Up
4:66172555|66200637	7.55994991	0.00491396	0.03931169	Up
2:238023879|238038227	−7.4844817	0.02717724	0.04348359	Down
2:188269009|188286112	7.37184575	0.02982719	0.04338501	Up
14:37238505|37262083	7.19293915	0.0351073	0.04320898	Up
9:11209034|11219449	7.09676658	0.00938513	0.03754053	Up
5:161794861|161799241	−6.3887762	0.02483465	0.0496693	Down
4:58367537|58420865	−6.3779976	0.02537228	0.04510628	Down

enriched in biological regulation and metabolic process among biological process (BP) categories, in membrane and nucleus among cellular component (CC) categories, as well as in protein binding and ion binding among molecular function (MF) categories (Figure S6A). We also determined top 20 enriched BP terms of the lncRNA-associated ceRNA network (Figure 5A) and circRNA-associated ceRNA network (Figure 5B). We found that mRNAs in the lncRNA-associated ceRNA network were positively correlated with ERK1 and ERK2 cascade, cell-cell adhesion and regulation of cellular response to stress, while negatively correlated with response to oxidative stress, response to interleukin-1 and ncRNA metabolic process. On the other hand, mRNAs in the circRNA-associated ceRNA network were positively correlated with Ras and cGMP-PKG signaling pathways, while negatively correlated with MAPK and NF-κB signaling pathways. Top 20 enriched CC (Figure S6B) and MF (Figure S6C) terms of icariin-associated ceRNA networks were also demonstrated.

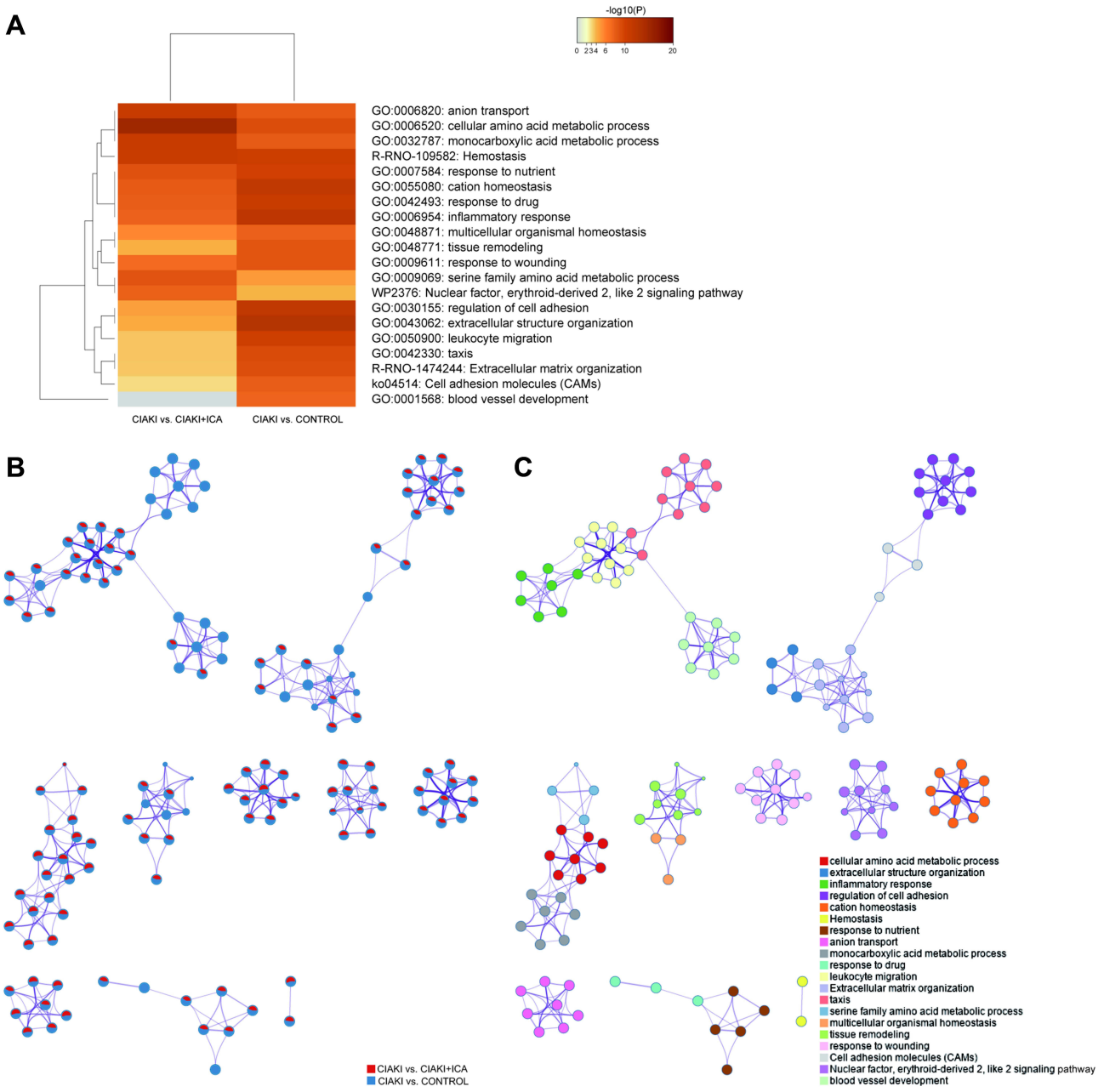

Figure 4 Function annotation of DEGs in CIAKI rats. (**A**) The enriched ontology clusters were demonstrated by a heatmap. The heatmap cells were colored by their *p* values. (**B** and **C**) The enriched ontology clusters were displayed by a network. (**B**) Each term is represented by a pie, where the pie sector is proportional to the number of genes from an individual group. (**C**) Each term is represented by a circle node, where its size is proportional to the number of genes that fall into an individual term, and its color represents its cluster identity.

Using an online tool String, we also investigated the protein–protein interaction of mRNAs in icariin-associated ceRNA networks (Figure 5C). Interestingly, Map3k14, a canonical NF-κB signaling inducing kinase, was involved in hub genes of the PPI network, as well as Utp15, Epha4 and Rps3.

Identification and Validation of Key Modules in Icariin-Associated ceRNA Networks

To find out key modules of the icariin associated ceRNA networks, the "Cytohubba" plug-in of Cytoscape software was applied. Combining seven methods in "Cytohubba" (betweenness, mcc, closeness, degree, epc, radiality and stress), we figured out a hub lncRNA-associated ceRNA network with 4 miRNAs (rno-miR-146b-5p, rno-miR-339-5p, rno-miR

Table 5 Top 10 Enriched GO Terms of DEGs

GO	Category	Description	Gene Count	%	$Log_{10}(P)$	$Log_{10}(q)$
CONTROL vs CIAKI						
GO:0043062	GO Biological Processes	Extracellular structure organization	72	4.4	−13	−9.3
GO:0045229	GO Biological Processes	External encapsulating structure organization	72	4.4	−13	−9.3
GO:0030198	GO Biological Processes	Extracellular matrix organization	71	4.3	−13	−9.1
GO:0006954	GO Biological Processes	Inflammatory response	127	7.7	−12	−8.7
GO:0030155	GO Biological Processes	Regulation of cell adhesion	132	8	−12	−8.6
GO:0055080	GO Biological Processes	Cation homeostasis	134	8.1	−12	−8.6
GO:0055065	GO Biological Processes	Metal ion homeostasis	125	7.6	−12	−8.6
GO:0072507	GO Biological Processes	Divalent inorganic cation homeostasis	105	6.4	−12	−8.6
GO:0006873	GO Biological Processes	Cellular ion homeostasis	124	7.5	−12	−8.4
GO:0042493	GO Biological Processes	Response to drug	113	6.9	−11	−7.8
CIAKI vs CIAKI+ICA						
GO:0006520	GO Biological Processes	Cellular amino acid metabolic process	61	4.6	−15	−11
GO:1901605	GO Biological Processes	Alpha-amino acid metabolic process	48	3.6	−14	−10
GO:0006820	GO Biological Processes	Anion transport	86	6.5	−11	−7.9
GO:0032787	GO Biological Processes	Monocarboxylic acid metabolic process	95	7.1	−11	−7.9
R-RNO-109582	Reactome Gene Sets	Hemostasis	74	5.6	−11	−7.8
GO:0016053	GO Biological Processes	Organic acid biosynthetic process	56	4.2	−10	−7.3
GO:0046394	GO Biological Processes	Carboxylic acid biosynthetic process	54	4.1	−9.4	−6.6
R-RNO-71291	Reactome Gene Sets	Metabolism of amino acids and derivatives	44	3.3	−9.2	−6.4
GO:0016054	GO Biological Processes	Organic acid catabolic process	45	3.4	−9	−6.2
GO:0015711	GO Biological Processes	Organic anion transport	63	4.7	−8.9	−6.2

-345-3p and rno-miR-6328), 6 lncRNAs (MSTRG.34520.3, MSTRG.4074.10, MSTRG.51241.14, MSTRG.51241.15, MSTRG.69307.1 and MSTRG.71029.16) and 6 mRNAs (Acot1, Ly6i, Map3k14, Mettl2, Set and Tmem44). We also set up a hub circRNA-associated ceRNA network with 1 miRNA (rno-miR-339-5p), 2 circRNAs (10:13767446|13810899 and 3:177390074|177433646) and 8 mRNAs (Acot1, Cbwd1, Ly6i, Map3k14, Mettl2, Nyap1, Set and Utp20). An overview of the hub ceRNA network was also demonstrated by a Sankey plot (Figure 6A). Detail of each hub gene is presented in Tables 6 and 7.

Further, we detected the expressions of above 9 mRNAs involved in the icariin-associated ceRNA network by PCR analysis. As shown in Figure 6B, CM induced significant elevation of Acot1, Map3k14 and Ly6i, which could be reversed by icariin pretreatment. Icariin pretreatment also attenuated CM-induced expressions of Mettl2 and Set.

From the hub ceRNA networks, we focused on the overlapped mRNA Map3k14. Based on the level of Map3k14 in the nine sequenced rat kidneys, we carried out GSEA analysis. We could see from Figure S7, mRNA metabolic process (NES = 2.332, $p < 0.001$), ncRNA metabolic process (NES = 2.996, $p < 0.001$) and apoptotic signaling pathway (NES = 2.257, $p < 0.001$) were positively enriched.

Relationship of Icariin-Associated ceRNA Networks and Renal Function

Finally, we tried to inspect the relationship between the key modules of ceRNA networks and renal function. Using an R package "corrplot", Figure 7A and Figure S8 were drawn to demonstrate the correlation of 21 key modules and renal function (Cr, BUN and Cys-C). Three biomarkers of renal function showed similar trends of correlation with the key modules. They were negatively correlated with one mRNA (Tmem44), one miRNA (rno-miR-339-5p) and one lncRNA (MSTRG.4074.10). On the other hand, they were positively correlated with eight mRNAs (Acot1, Cbwd1, Ly6i,

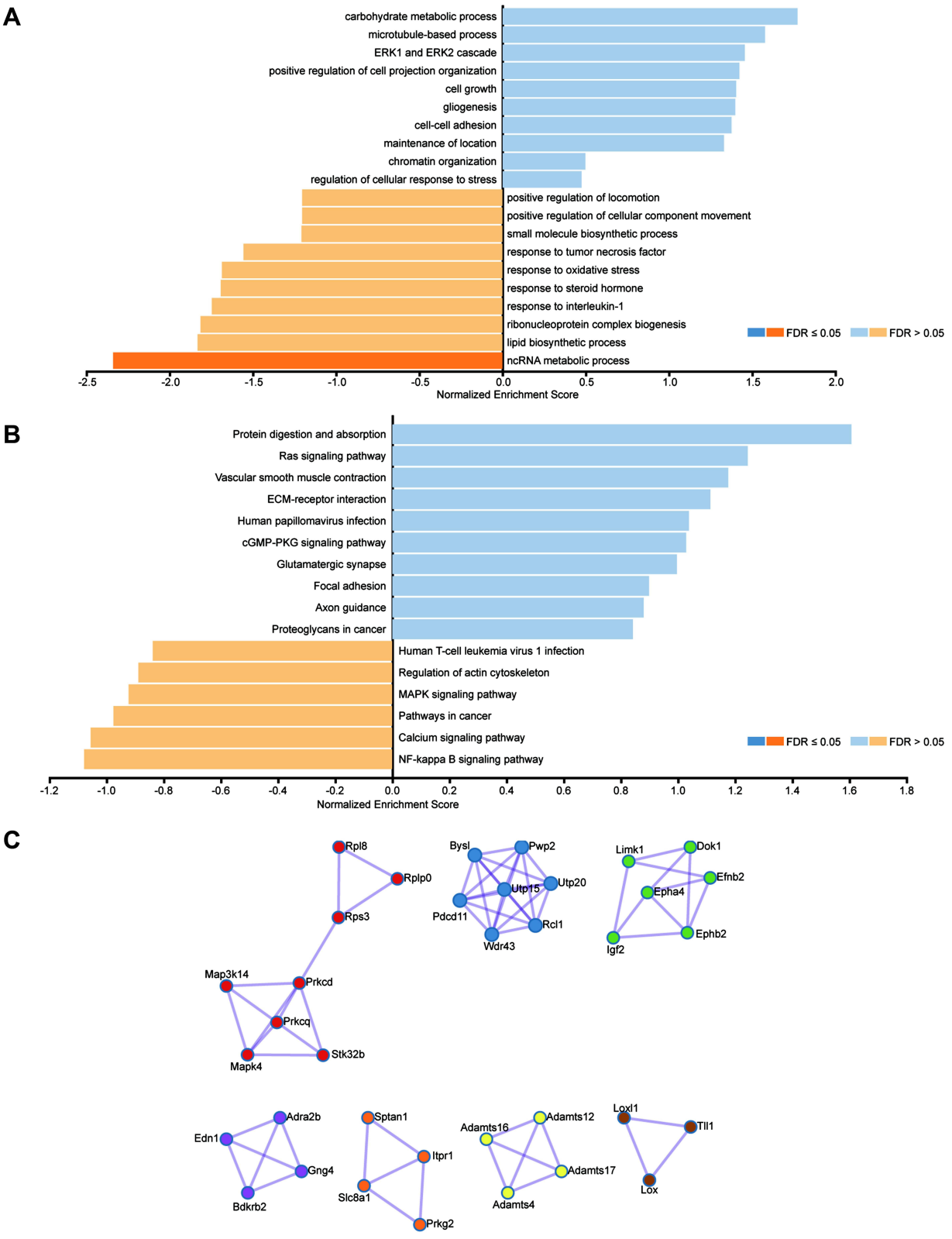

Figure 5 Function annotation and PPI of DEGs in the ceRNA network. (**A**) The most significant BP terms of GO analysis for DEGs in the lncRNA-associated ceRNA network. (**B**) The most significant BP terms of GO analysis for DEGs in the circRNA-associated ceRNA network. Blue bars stand for positive association between the individual BP term and icariin pretreatment. Yellow bars stand for negative association between the individual BP term and icariin pretreatment. (**C**) The protein–protein interaction network of DEGs in the ceRNA networks, calculated by MCODE algorithm.

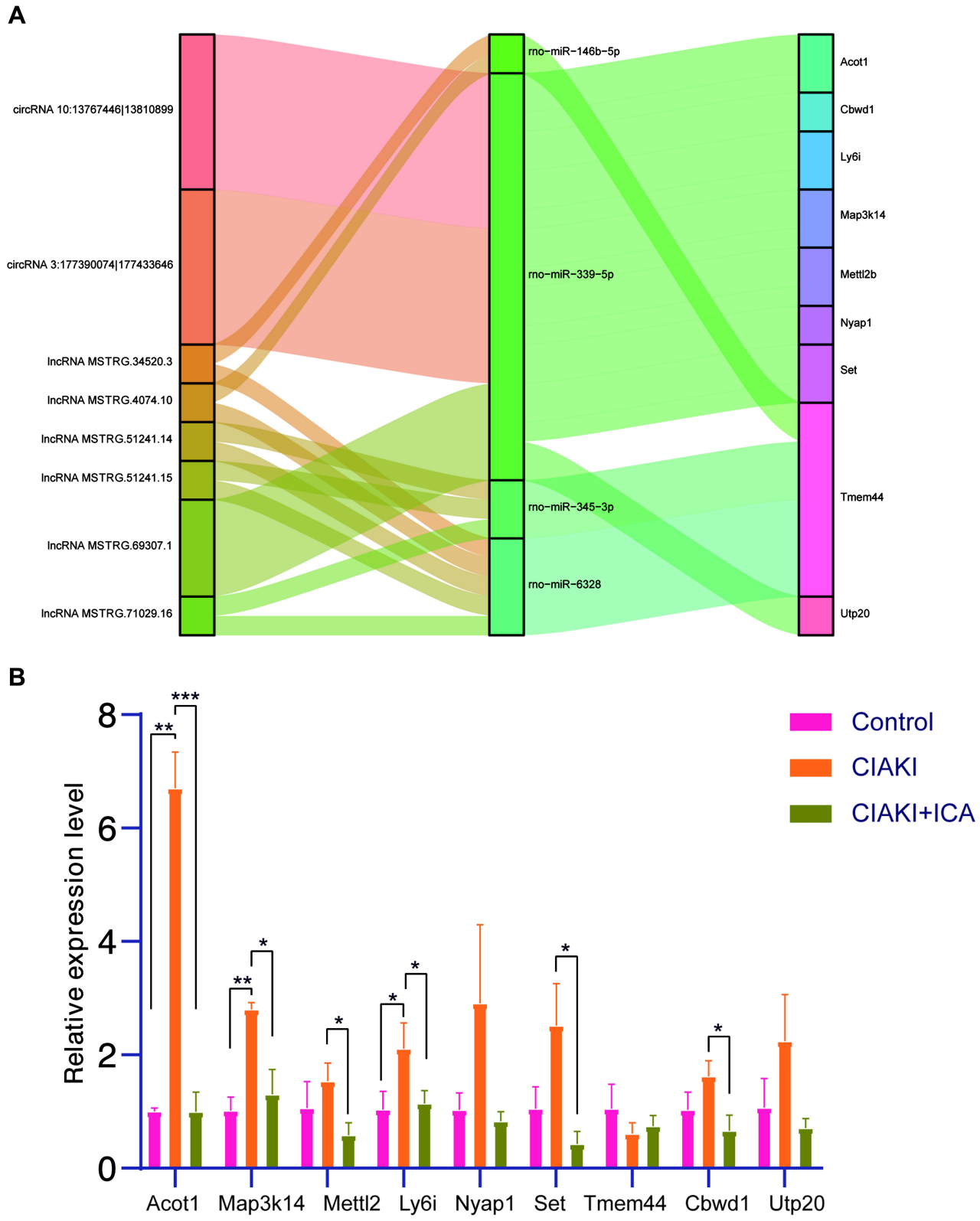

Figure 6 Hub genes of the ceRNA network in icariin pretreated CIAKI rats. Hub genes of icariin-associated ceRNA network were displayed by Sankey plot (**A**). The expressions of hub mRNAs were examined by PCR in control group, CIAKI group and CIAKI+icariin group (**B**). *$p < 0.05$; **$p < 0.01$; ***$p < 0.001$.

Table 6 Hub Nodes of lncRNA-Associated ceRNA Analysis

Name	Degree	Betweeness	Closeness	Radiality
lncRNA				
MSTRG.34520.3	2	1445.989	80.83333	3.17067
MSTRG.4074.10	2	1445.989	80.83333	3.17067
MSTRG.51241.14	2	2099.137	85.11667	3.212015
MSTRG.51241.15	2	2099.137	85.11667	3.212015
MSTRG.69307.1	2	3442.797	76.53333	3.016216
MSTRG.71029.16	2	2099.137	85.11667	3.212015
microRNA				
rno-miR-146b-5p	25	11,401.44	80.05	3.090563
rno-miR-339-5p	99	27,805.36	126.3	3.336705
rno-miR-345-3p	46	14,196.37	93.26667	3.173254
rno-miR-6328	105	28,717.1	132.85	3.483344
mRNA				
Acot1	2	1657.999	78.16667	3.062739
Ly6i	2	1657.999	78.16667	3.062739
Map3k14	2	1657.999	78.16667	3.062739
Mettl2	2	1657.999	78.16667	3.062739
Set	2	1657.999	78.16667	3.062739
Tmem44	2	2099.137	85.11667	3.212015

Table 7 Hub Nodes of circRNA-Associated ceRNA Analysis

Name	Degree	Betweeness	Closeness	Radiality
circRNA				
10:13767446|13810899	2	878.9485	64.83333	2.54382
3:177390074|177433646	3	2992.215	65.75	2.559075
microRNA				
rno-miR-339-5p	91	18,178.16317	110.1667	2.967154
mRNA				
Acot1	2	298.2639	62.58333	2.475171
Cbwd1	2	581.9124	64.33333	2.528565
Ly6i	2	298.2639	62.58333	2.475171
Map3k14	2	298.2639	62.58333	2.475171
Mettl2	2	298.2639	62.58333	2.475171
Nyap1	2	878.9485	64.83333	2.54382
Set	2	298.2639	62.58333	2.475171
Utp20	2	878.9485	64.83333	2.54382

Map3k14, Mettl2, Nyap1, Set and Utp20), two miRNAs (rno-miR-345-3p and rno-miR-6328), one lncRNA (MSTRG.69307.1) and one circRNA (10:13767446|13810899).

More specifically, fitting curves of Cr and key modules were exhibited. Acot1 (Figure 7B, $p < 0.001$), Cbwd1 (Figure 7C, $p < 0.001$), Map3k14 (Figure 7D, $p = 0.02$), Nyap1 (Figure 7E, $p < 0.001$), rno-miR-6328 (Figure 7H, $p = 0.001$) and lncRNA MSTRG.69307.1 (Figure 7J, $p = 0.02$) were positively correlated with Cr level. Meanwhile, Tmem44 (Figure 7F, $p = 0.007$), rno-miR-339-5p (Figure 7G, $p = 0.003$) and lncRNA MSTRG.4074.10 (Figure 7I, $p = 0.004$) were negatively correlated with Cr level.

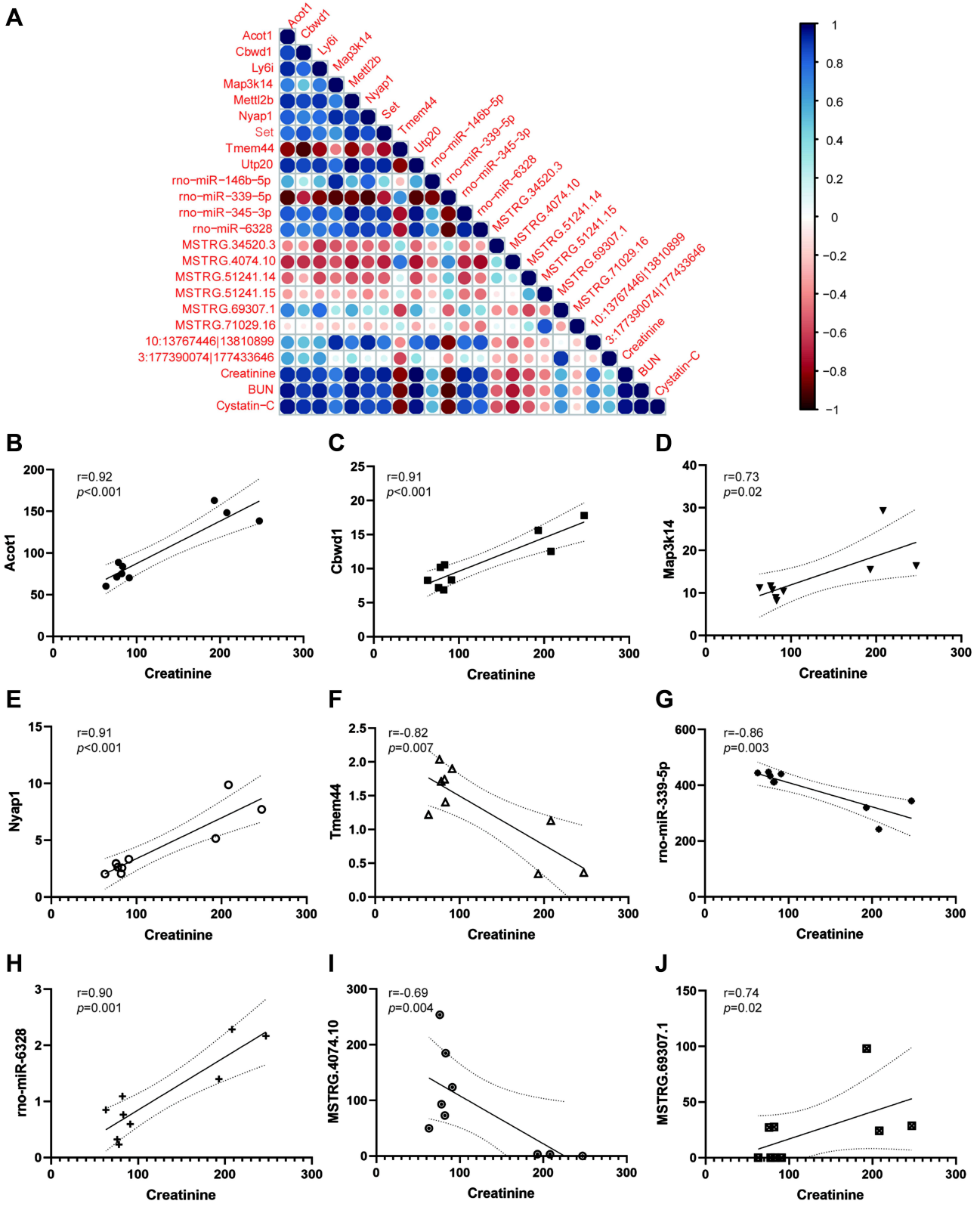

Figure 7 Association of hub genes in the ceRNA network and renal function. (**A**) Correlation analysis of hub genes in the ceRNA network and biomarkers of renal function (Cr, BUN and Cys-C). The red dots stand for positive correlation, and the blue dots stand for negative correlation. The size and darkness stand for the strength of correlation. A darker and larger dot stands for stronger correlation. The fitting curves for Cr and specific hub genes (Acot1(**B**), Cbwd1 (**C**), Map3k14 (**D**), Nyap1 (**E**), Tmem44 (**F**), rno-miR-339-5p (**G**), rno-miR-6328 (**H**), MSTRG.4074.10 (**I**), MSTRG.69307.1(**J**)) were also presented. The straight line shows the fitting curve and the dotted line demonstrates 95% confidence interval.

Discussion

In the present study, we reported the protective effect of icariin against CIAKI. We also demonstrated the expression profiles and function annotation of mRNAs, miRNAs, lncRNAs and circRNAs in icariin pretreated CIAKI rat kidneys. Further, we figured out an icariin-associated ceRNA network and evaluated its relationship with renal function.

The pathophysiological mechanisms of CIAKI have not been thoroughly elucidated, but direct nephrotoxic effect of CM and disturbance of renal blood flow have been generally recognized.[5,23] CM are toxic to the tubular epithelium, leading to inflammation and apoptosis. With progressed cellular injury, tubular epithelial cells detach from the basement membrane and cause luminal obstruction, and finally cause a decrease of glomerular filtration rate.[5] Disturbed renal blood flow can cause arteriolar vasoconstriction and microvascular thrombosis, which enhance the renal tubular injury. Therefore, preventive strategies targeting the above pathogenesis may be effective. In this study, icariin significantly protected against CM-induced renal tubular apoptosis, as a profound decrease in numbers of TUNEL-positive tubular cells was observed. Function annotation of DEGs showed an enrichment of inflammatory response, regulation of cell adhesion, leukocyte migration and blood vessel development in icariin pretreated CIAKI rats. Similarly, Xie et al reported a protection of icariin against inflammatory response, apoptosis and vascular permeability in a sepsis-induced AKI mouse model.[24] In another unilateral ureteral obstruction mouse model, icariin also mitigated several proinflammatory factors, such as NF-κB, cyclooxygenase-2 and interleukin 1β.[10] Thus, the universal anti-inflammation and anti-apoptosis effect of icariin may contribute to its remarkable protection in CIAKI model, as the improved renal function and alleviated histological injury were demonstrated in our study. To our knowledge, this is the first report about the protective effect of icariin against CIAKI.

Then, we focused on the potential role of ncRNAs in icariin protection against CIAKI. ncRNAs, as important epigenetic modulators, can induce changes to a phenotype without influencing a genotype. They are potentially reversible and can be affected by environmental factors, age and disease state. Emerging evidence suggests a crucial role of ncRNAs in various kidney diseases, such as AKI, CKD, diabetic kidney disease and renal carcinoma. For example, Lorenzen et al demonstrated elevation of three novel circRNAs in blood of patients with AKI, among which circR-126 might play as a predictor of mortality.[25] LncRNA H19, elevated in kidney biopsies of patients with AKI and in murine ischemic kidney tissues was shown to attenuate ischemic AKI by sponging miRNA-30a-5p.[26] In the present study, we found 128 DE miRNAs, 989 DE lncRNAs and 16 DE circRNAs between CIAKI and CIAKI+icariin group. Particularly, rno-miR-339-5p was up-regulated in CIAKI+icariin group, while rno-miR-146b-5p and rno-miR-345-3p were down-regulated. MiR-339-5p was proven to be associated with risk of end stage kidney disease in diabetic patients.[27] In glomerular mesangial cells, miR-146b-5p attenuated the inflammatory response by inhibiting Toll-like receptor 4 pathway in lupus nephritis.[28] MiR-345-3p also presented significant pathological relevance in cardiorenal syndrome.[29] Focused on so many popular ncRNAs, we were also curious about the underlying mechanism and interaction of these ncRNAs in icariin protection against CIAKI.

The foundation of ceRNA hypothesis is that both coding and non-coding endogenous RNA molecules sharing miRNA response elements (MREs) can competitively prevent the action of miRNAs on their mRNA targets, thereby regulate gene expression in trans.[30] A variety of experiments have proven the crucial role of ceRNA networks in AKI. For example, a ceRNA axis involving lncRNA TCONS_00016233, miR-22-3p and AIFM1 contributed to TLR4/MAPK signal pathway and enhanced septic AKI.[31] Bao et al constructed a ceRNA network including 22 lncRNAs, 5 miRNAs and 37 mRNAs in a CIAKI rat model, which was functionally enriched in cell adhesion molecules (rno04514), intracellular signal transduction (GO:0035556) and transmembrane transporter activity (GO:0022857).[16] In another study focused on CIAKI, Cheng et al demonstrated a ceRNA network involving 38 circRNAs, 12 lncRNAs, 13 miRNAs and 127 mRNAs.[32] Further function annotation of that study presented an enrichment in TNF signaling pathway (rno04668), RNA splicing and nucleoside binding. In our study, based on the DEGs between CIAKI group and CIAKI+icariin group, we constructed a lncRNA-associated ceRNA network (including 93 lncRNAs, 15 miRNAs and 281 mRNAs) and a circRNA-associated ceRNA network (including 4 circRNAs, 8 miRNAs and 252 mRNAs). Similarly, mRNAs in the ceRNA networks were remarkably enriched in ncRNA metabolic process, cell-cell adhesion and several canonical signal pathways (MAPK signaling, NF-κB signaling, calcium signaling, ERK1 and ERK2

cascade). Our results indicated that the function of ceRNA network in icariin protection against CIAKI might consist with that in CIAKI pathogenesis, or even with that in other AKI models. Moreover, we identified 21 key modules (involving 6 lncRNAs, 2 circRNAs, 4 miRNAs and 9 mRNAs) in these ceRNA networks, which might be highly correlated with the protective effect of icariin in CIAKI. Interestingly, rno-miR-339-5p, rno-miR-345-3p and rno-miR -146b-5p were among top 5 hub genes in the 22 key modules. Additionally, rno-miR-339-5p showed negative correlation with rats' Cr level, while rno-miR-345-3p and rno-miR-146b-5p showed positive correlation. As mentioned above, these three miRNAs all presented relevance with pathogenesis and prognosis in other kidney diseases, which prompted a crucial role of ceRNA networks in icariin protection against CIAKI.

Map3k14, an NF-κB inducing kinase, showed up as a core gene in the mechanism of icariin protection against CIAKI in the present study. It was among the hub genes both in the ceRNA network and in the PPI network, and it was associated with deteriorating renal function. ncRNA and mRNA metabolism, as well as apoptotic signaling, were all highly correlated with Map3k14 expression pattern. Consistently, Map3k14 has been proven to promote inflammation and cell death in acute folate nephropathy.[33] Map3k14 overexpression increased inflammatory cytokines such as IL-6, IL-8 and MCP-1 in cultured human proximal tubular cells.[34] Mechanistically, Map3k14 functions by regulation of both canonical and non-canonical NF-κB pathways, as well as NF-κB-independent actions (such as regulation of transcription factor activity and epigenetic mechanism).[35] These might account for the underlying mechanism of icariin protection in CIAKI partially, as the icariin-associated ceRNA network was also enriched in ncRNA metabolism and NF-κB signaling.

Despite these thought-provoking results, there are certain limitations of our study. First, we selected three rat kidneys in each group for sequencing analysis. Further experiments with a larger number of samples and a greater variety of tissue, including more precise renal medulla and cortex, are needed for sequencing analysis. Second, we only focused on the kidney injury induced by one type of CM—iopromide. Therefore, we will discuss the effect of icariin in CIAKI models induced by different CM. Third, we did not verify ceRNA network in the in vitro CIAKI models, which should be covered in the future. Finally, we did not involve human samples in the present study. We will collect patients' blood and kidney samples for further investigation to increase persuasion of the study.

Conclusion

In the current study, we reported, for the first time, the protective effect of icariin in CIAKI via both in vivo and in vitro studies. The ceRNA network based on high-throughput sequencing revealed that Acot1, Cbwd1, Ly6i, Map3k14, Mettl2, Nyap1, Set, Tmem44 and Utp20 were crucial genes in icariin action. The lncRNA/circRNA-miRNA-mRNA interaction further prompted that ERK1 and ERK2 cascade, MAPK signaling and NF-κB signaling might take part in the icariin protection against CIAKI. The above results may shed a light on succeeding studies about the preventive strategies of CIAKI.

Abbreviations

AKI, acute kidney injury; ANOVA, analysis of variance; BUN, blood urea nitrogen; CC, cellular component; CCK-8, cell counting kit-8; ceRNA, competing endogenous RNA; CIAKI, contrast induced acute kidney injury; circRNA, circular RNA; CM, contrast medium; Cr, creatinine; Cys-C, Cystatin C; DE, differentially expressed; DEG, differentially expressed genes; FC, fold change; GO, gene ontology; HE, hematoxylin and eosin; lncRNA, long non-coding RNA; LSD, least significant difference; MF, molecular function; miRNA, microRNA; MRE, miRNA response element; ncRNA, non-coding RNA; PAS, Periodic Acid-Schiff; PPI, protein–protein interaction; TPM, transcripts per million.

Data Sharing Statement

The datasets generated and analyzed during current study are available in the GEO repository [GSE189881].

Ethics Approval and Consent to Participate

All animal experiments were approved by Guangzhou Medical University and conducted in accordance with the US guidelines (NIH publication #85-23, revised in 1985).

Funding

This work was supported by National Natural Science Foundation of China (grant numbers 82000355 and 81902831), Guangdong Provincial Natural Science Foundation (grant number 2021A1515111114), Guangzhou Science and Technology Program (grant numbers 202102080037 and 202102020831), Guangzhou Traditional Chinese Medicine and Integrated Medicine Technology Program (grant number 20212A11023) and Scientific research funding of Traditional Chinese Medicine Bureau of Guangdong Province (grant number 20221246).

Disclosure

The authors declare that they have no competing interests.

References

1. Azzalini L, Spagnoli V, Ly HQ. Contrast-induced nephropathy: from pathophysiology to preventive strategies. *Can J Cardiol*. 2016;32(2):247–255. doi:10.1016/j.cjca.2015.05.013
2. Kellum JA, Lameire N. Diagnosis, evaluation, and management of acute kidney injury: a KDIGO summary (Part 1). *Critical Care*. 2013;17(1):204. doi:10.1186/cc11454
3. Shema L, Ore L, Geron R, Kristal B. Contrast-induced nephropathy among Israeli hospitalized patients: incidence, risk factors, length of stay and mortality. *Isr Med Assoc J*. 2009;11(8):460–464.
4. Yan L, Jiaqiong L, Yue G, et al. Atorvastatin protects against contrast-induced acute kidney injury via upregulation of endogenous hydrogen sulfide. *Ren Fail*. 2020;42(1):270–281. doi:10.1080/0886022x.2020.1740098
5. Mehran R, Dangas GD, Weisbord SD. Contrast-associated acute kidney injury. *N Engl J Med*. 2019;380(22):2146–2155. doi:10.1056/NEJMra1805256
6. Nijssen EC, Rennenberg RJ, Nelemans PJ, et al. Prophylactic hydration to protect renal function from intravascular iodinated contrast material in patients at high risk of contrast-induced nephropathy (AMACING): a prospective, randomised, Phase 3, controlled, open-label, non-inferiority trial. *Lancet*. 2017;389(10076):1312–1322. doi:10.1016/s0140-6736(17)30057-0
7. Sze SC, Tong Y, Ng TB, Cheng CL, Cheung HP. Herba Epimedii: anti-oxidative properties and its medical implications. *Molecules*. 2010;15(11):7861–7870. doi:10.3390/molecules15117861
8. Li C, Li Q, Mei Q, Lu T. Pharmacological effects and pharmacokinetic properties of icariin, the major bioactive component in Herba Epimedii. *Life Sci*. 2015;126:57–68. doi:10.1016/j.lfs.2015.01.006
9. Zhou YD, Hou JG, Yang G, et al. Icariin ameliorates cisplatin-induced cytotoxicity in human embryonic kidney 293 cells by suppressing ROS-mediated PI3K/Akt pathway. *Biomed Pharmacother*. 2019;109:2309–2317. doi:10.1016/j.biopha.2018.11.108
10. Chen HA, Chen CM, Guan SS, Chiang CK, Wu CT, Liu SH. The antifibrotic and anti-inflammatory effects of icariin on the kidney in a unilateral ureteral obstruction mouse model. *Phytomedicine*. 2019;59:152917. doi:10.1016/j.phymed.2019.152917
11. Jia Z, Wang K, Zhang Y, et al. Icariin ameliorates diabetic renal tubulointerstitial fibrosis by restoring autophagy via regulation of the miR-192-5p/GLP-1R pathway. *Front Pharmacol*. 2021;12:720387. doi:10.3389/fphar.2021.720387
12. Wang M, Wang L, Zhou Y, Feng X, Ye C, Wang C. Icariin attenuates renal fibrosis in chronic kidney disease by inhibiting interleukin-1β/transforming growth factor-β-mediated activation of renal fibroblasts. *Phytother Res*. 2021;35:6204–6215. doi:10.1002/ptr.7256
13. Qi MY, He YH, Cheng Y, et al. Icariin ameliorates streptozocin-induced diabetic nephropathy through suppressing the TLR4/NF-κB signal pathway. *Food Funct*. 2021;12(3):1241–1251. doi:10.1039/d0fo02335c
14. Haddad G, Kölling M, Wegmann UA, et al. Renal AAV2-mediated overexpression of long non-coding RNA H19 attenuates ischemic acute kidney injury through sponging of microRNA-30a-5p. *J Am Soc Nephrol*. 2021;32(2):323–341. doi:10.1681/asn.2020060775
15. Thomson DW, Dinger ME. Endogenous microRNA sponges: evidence and controversy. *Nat Rev Genet*. 2016;17(5):272–283. doi:10.1038/nrg.2016.20
16. Bao W, Xiao Z, Wang Z, Liu D, Tan P, Huang M. Comprehensive analysis of the long non-coding RNA expression profile and functional roles in a contrast-induced acute kidney injury rat model. *Exp Ther Med*. 2021;22(1):739. doi:10.3892/etm.2021.10171
17. Zhang X, Chen Y, Zhang C, et al. Effects of icariin on the fracture healing in young and old rats and its mechanism. *Pharm Biol*. 2021;59(1):1245–1255. doi:10.1080/13880209.2021.1972121
18. Zhang W, Yuan W, Xu N, Li J, Chang W. Icariin improves acute kidney injury and proteinuria in a rat model of pregnancy-induced hypertension. *Mol Med Rep*. 2017;16(5):7398–7404. doi:10.3892/mmr.2017.7513
19. Liu Y, Liu B, Liu Y, et al. MicroRNA expression profile by next-generation sequencing in a novel rat model of contrast-induced acute kidney injury. *Ann Transl Med*. 2019;7(8):178. doi:10.21037/atm.2019.04.44
20. Weidemann A, Bernhardt WM, Klanke B, et al. HIF activation protects from acute kidney injury. *J Am Soc Nephrol*. 2008;19(3):486–494. doi:10.1681/asn.2007040419
21. Li J, Xu S, Zhu JB, et al. Pretreatment with cholecalciferol alleviates renal cellular stress response during ischemia/reperfusion-induced acute kidney injury. *Oxid Med Cell Longev*. 2019;2019:1897316. doi:10.1155/2019/1897316
22. Szklarczyk D, Gable AL, Lyon D, et al. STRING v11: protein-protein association networks with increased coverage, supporting functional discovery in genome-wide experimental datasets. *Nucleic Acids Res*. 2019;47(D1):D607–d13. doi:10.1093/nar/gky1131
23. Tan X, Zheng X, Huang Z, Lin J, Xie C, Lin Y. Involvement of S100A8/A9-TLR4-NLRP3 inflammasome pathway in contrast-induced acute kidney injury. *Cell Physiol Biochem*. 2017;43(1):209–222. doi:10.1159/000480340
24. Xie C, Liu L, Wang Z, et al. Icariin improves sepsis-induced mortality and acute kidney injury. *Pharmacology*. 2018;102(3–4):196–205. doi:10.1159/000487955

25. Kölling M, Seeger H, Haddad G, et al. The circular RNA ciRs-126 predicts survival in critically ill patients with acute kidney injury. *Kidney Int Rep*. 2018;3(5):1144–1152. doi:10.1016/j.ekir.2018.05.012
26. He Y, Lang X, Cheng D, Zhang T, Yang Z, Xiong R. miR-30a-5p inhibits hypoxia/reoxygenation-induced oxidative stress and apoptosis in HK-2 renal tubular epithelial cells by targeting glutamate dehydrogenase 1 (GLUD1). *Oncol Rep*. 2020;44(4):1539–1549. doi:10.3892/or.2020.7718
27. Satake E, Saulnier PJ, Kobayashi H, et al. Comprehensive search for novel circulating miRNAs and axon guidance pathway proteins associated with risk of ESKD in diabetes. *J Am Soc Nephrol*. 2021;32(9):2331–2351. doi:10.1681/asn.2021010105
28. Sheng ZX, Yao H, Cai ZY. The role of miR-146b-5p in TLR4 pathway of glomerular mesangial cells with lupus nephritis. *Eur Rev Med Pharmacol Sci*. 2018;22(6):1737–1743. doi:10.26355/eurrev_201803_14589
29. Ishrat R, Ahmed MM, Tazyeen S, et al. In silico integrative approach revealed key MicroRNAs and associated target genes in cardiorenal syndrome. *Bioinform Biol Insights*. 2021;15:11779322211027396. doi:10.1177/11779322211027396
30. Salmena L, Poliseno L, Tay Y, Kats L, Pandolfi PP. A ceRNA hypothesis: the Rosetta stone of a hidden RNA language? *Cell*. 2011;146(3):353–358. doi:10.1016/j.cell.2011.07.014
31. Zhang P, Yi L, Qu S, et al. The biomarker TCONS_00016233 drives septic AKI by targeting the miR-22-3p/AIFM1 signaling axis. *Mol Ther Nucleic Acids*. 2020;19:1027–1042. doi:10.1016/j.omtn.2019.12.037
32. Cheng W, Li XW, Xiao YQ, Duan SB. Non-coding RNA-associated ceRNA networks in a new contrast-induced acute kidney injury rat model. *Mol Ther Nucleic Acids*. 2019;17:102–112. doi:10.1016/j.omtn.2019.05.011
33. Ortiz A, Husi H, Gonzalez-Lafuente L, et al. Mitogen-activated protein kinase 14 promotes AKI. *J Am Soc Nephrol*. 2017;28(3):823–836. doi:10.1681/asn.2015080898
34. Zhao Y, Banerjee S, LeJeune WS, Choudhary S, Tilton RG. NF-κB-inducing kinase increases renal tubule epithelial inflammation associated with diabetes. *Exp Diabetes Res*. 2011;2011:192564. doi:10.1155/2011/192564
35. Valiño-Rivas L, Vaquero JJ, Sucunza D, et al. NIK as a druggable mediator of tissue injury. *Trends Mol Med*. 2019;25(4):341–360. doi:10.1016/j.molmed.2019.02.005